



# Glaser Coupling at Metal Surfaces\*\*

Hong-Ying Gao, Hendrik Wagner, Dingyong Zhong, Jörn-Holger Franke, Armido Studer,\* and Harald Fuchs\*

The direct “bottom-up” preparation of innovative nano-scaled systems at surfaces is of great interest because of the potential applications in materials science and molecular electronics.<sup>[1]</sup> In this regard, on-surface synthesis, by which defined nanostructures are constructed at surfaces through the covalent coupling of organic precursor molecules, is a key technology that constitutes a young research field. Such processes (two-dimensional or 2D reactions) are generally carried out under ultra-high-vacuum (UHV) conditions and the success of the reaction is conveniently monitored by scanning tunneling microscopy (STM). Using this approach the synthesis of robust functional materials that cannot be prepared by “classical” solution-phase synthesis is possible.<sup>[1a]</sup> To date, the most frequently applied 2D reaction is the Ullman coupling of aryl halides at various metal surfaces. Based on early contributions of Hla et al.,<sup>[2]</sup> Hecht and Grill developed a versatile process for the on-surface homocoupling of aryl bromides for the preparation of linear and 2D oligomers.<sup>[3]</sup> Müllen and Fasel further developed that surface reaction and successfully constructed conjugated polymeric materials and graphene nanoribbons.<sup>[4]</sup> A “state-of-the-art” application of the 2D Ullman coupling was reported by Hecht and Grill recently.<sup>[5]</sup> It was shown that orthogonal coupling of aryl bromides and iodides at the surface resulting in conjugated polymeric networks is possible. Besides Ullman coupling, other chemical reactions such as imine bond formation,<sup>[6]</sup> dehydration and esterification of boronic

acids,<sup>[7]</sup> thermal dimerization of N-heterocyclic carbenes,<sup>[8]</sup> and acylation reactions<sup>[9]</sup> have been applied at surfaces. By using a geometric constraint, the dehydrogenative coupling of inert alkanes at anisotropic Au(110) surfaces was recently achieved, which also convincingly demonstrates the potential of on-surface synthesis.<sup>[10]</sup>

Herein, we present the on-surface coupling of various arylalkynes (Glaser coupling),<sup>[11]</sup> which is halogen free and without “capping” ions, as an efficient 2D reaction at various metal surfaces (Scheme 1a). Arylalkynes are readily accessible starting materials and if the 2D Glaser coupling is conducted with bisethynylarenes (Scheme 1b), the resulting conjugated  $\pi$ -systems should show interesting physical properties.<sup>[12]</sup>

As monomers for initial investigations we chose the diethynyl-substituted  $\pi$ -system **1** (Figure 1a; for the preparation of **1** see the Supporting Information). We first studied the on-surface Glaser coupling of **1** on an Au(111) surface. Experiments were performed with an integrated UHV surface-analysis system equipped with an STM (Omicron). Compound **1** was deposited on an Au(111) surface at room temperature to form a clean monomolecular monolayer on

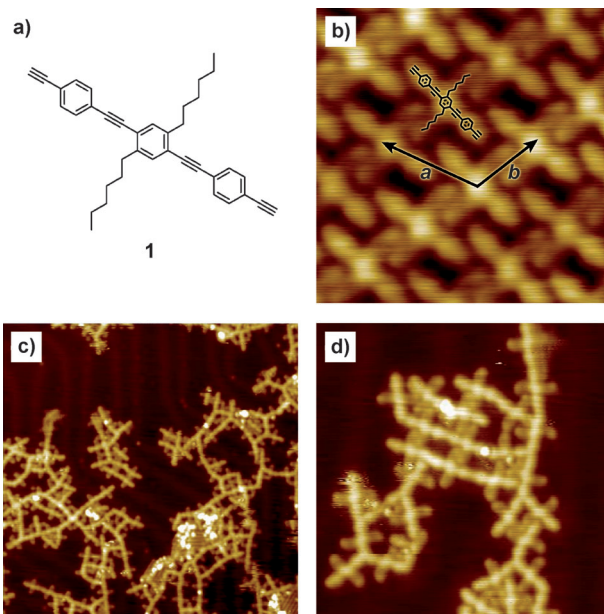


**Figure 1.** a) Molecular structure of alkyne **1**. b) High-resolution STM image of the adsorbed alkyne **1** on Au(111) (sample voltage  $-0.5$  V, tunnel current  $100$  pA,  $6$  nm  $\times$   $6$  nm). c) Oligomers formed from alkyne **1** on Au(111) after annealing at  $123$ – $140$  °C ( $-2$  V,  $20$  pA,  $40$  nm  $\times$   $40$  nm). d) High-resolution STM image of oligomers formed from alkyne **1** on Au(111) ( $-0.2$  V,  $10$  pA,  $15$  nm  $\times$   $15$  nm).

[\*] Dr. H.-Y. Gao,<sup>[†]</sup> Dr. D. Zhong, Dr. J.-H. Franke, Prof. Dr. H. Fuchs  
Physikalisches Institut  
Westfälische Wilhelms-Universität Münster  
Wilhelm-Klemm-Strasse 10, 48149 Münster (Germany)

and

Center for Nanotechnology  
Heisenbergstrasse 11, 48149 Münster (Germany)  
E-mail: fuchsh@uni-muenster.de

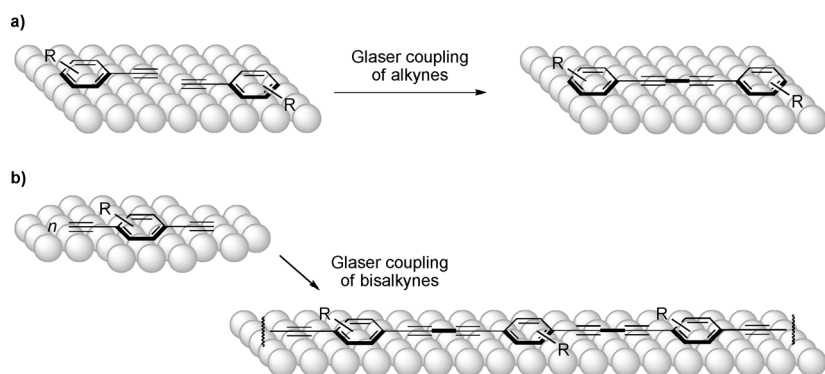
Prof. Dr. H. Fuchs  
Institute for Nanotechnology  
Karlsruhe Institute of Technology  
76344 Karlsruhe (Germany)  
Dr. H. Wagner,<sup>[†]</sup> Prof. Dr. A. Studer  
Organisch-Chemisches Institut  
Westfälische Wilhelms-Universität Münster  
Corrensstrasse 40, 48149 Münster (Germany)  
E-mail: studer@uni-muenster.de

[†] These authors contributed equally to this work.

[\*\*] We thank the Deutsche Forschungsgemeinschaft (SFB 858, TRR 61) for financial support and Prof. Lifeng Chi for helpful discussions. H.-Y.G. was supported by the Alexander von Humboldt-Foundation.



Supporting information for this article is available on the WWW under <http://dx.doi.org/10.1002/anie.201208597>.



**Scheme 1.** a) General outline of the 2D Glaser coupling at surfaces. b) On-surface Glaser coupling for the construction of conjugated chains.

the surface, as analyzed by UHV-STM (Figure 1b). The length of the molecule along the alkyne axis accounted for 2.43 nm and the length along the alkyl chains was 2.01 nm (periodic cell:  $a$  1.99 nm,  $b$  1.36 nm, angle  $116^\circ$ , as shown in Figure 1b). Subsequent annealing of the **1**-covered Au(111) surface (ca.  $125^\circ\text{C}$  for 30 min) led to oligomerization of **1** (formation of short chains) through the covalent coupling of the alkyne functionalities (Figure 1c; temperatures between  $123^\circ\text{C}$  and  $140^\circ\text{C}$  led to the same reaction outcome).

The success of the C–C bond formation was unambiguously proved by moving oligomers with the STM tip without destroying the connections between the individual monomer units (see the Supporting Information). Moreover, we compared the experimental center-to-center distance between two linked linear alkyne moieties with the theoretical bond length obtained by DFT calculations in the gas phase. The data are in good agreement (experimental value:  $2.36 \pm 0.02$  nm; theoretical value: 2.32 nm; see the Supporting Information). Therefore, an alternative conjugation mode where an Au atom links two alkyne moieties for which we calculated a center-to-center distance of 2.58 nm can be unambiguously excluded. Along with the targeted 2D Glaser coupling at surfaces, STM images also clearly indicated the occurrence of side reactions which led to chain branching (for further comparison of experimental and theoretical center-to-center distances see the Supporting Information). We identified several types of side reactions: apart from the desired Glaser coupling (Figure 2aI) we observed formal hydroalkynylation of the terminal alkyne functionality either at the  $\alpha$ - or  $\beta$ -position (Figure 2aII, aIII). We additionally observed the formation of diene products (Figure 2aIV) and hydroalkynylation also occurred at the Glaser product leading to an enediyne moiety (Figure 2aV). Interestingly, we also observed alkyne trimerization providing a branching point with an aromatic core structure (Figure 2aVI). Furthermore, two rare types of branching points with diene–diyne moieties could also be identified as others (see the Supporting Information).

For a more detailed study of the selectivity of the on-surface Glaser coupling we performed a statistical analysis with respect to the relative frequency of occurrence of the reaction pathways I–VI. To this end, we analyzed the connections between independent molecules and assigned

the successful bond-forming events to the different types of reactions (Figure 2).

Since it was not possible to unambiguously distinguish between reactions I and II, as well between IV and V in some cases, we combined the different reaction pathways to the pairs I/II and IV/V for the statistical analysis. However, it is important to note that within the I/II pair the main reaction type is the targeted linear homocoupling (I, Glaser reaction). The I/II pathways occurred with a proportion of  $(26 \pm 3)\%$  on average over four STM images analyzed (such as Figure 1c) on the Au(111) surface. Reaction pathway III could be identified with a frequency of  $(10.1 \pm 1.7)\%$  and pathways IV/V were most abundant, occurring with a frequency of  $(50 \pm 3.6)\%$ . The trimerization process (VI) occurred with a pro-

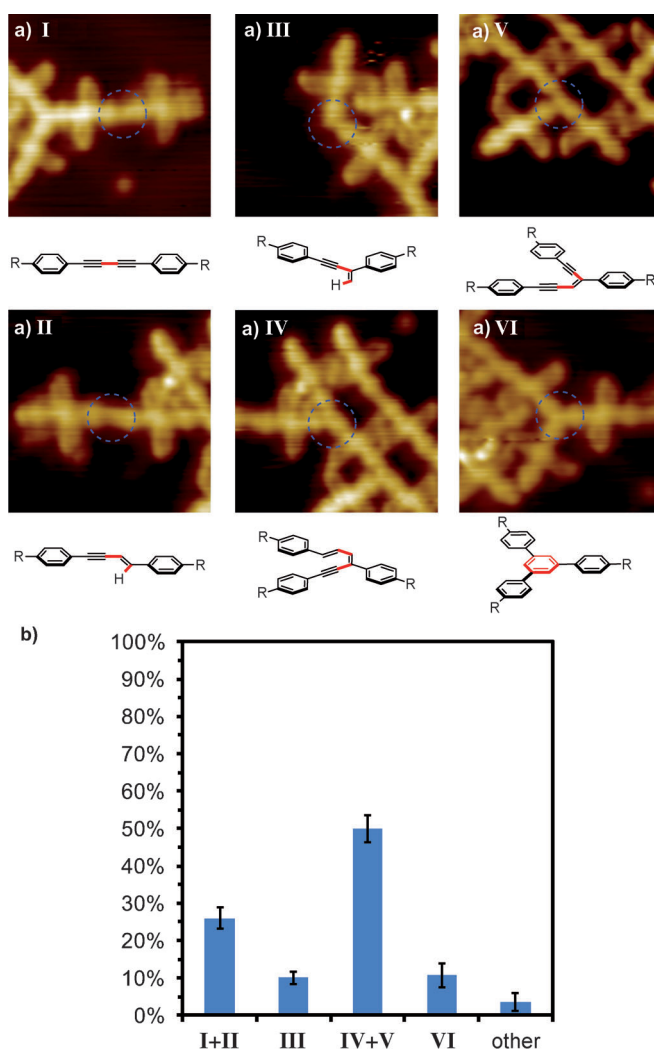


**Figure 2.** a) Overview of the STM images ( $-1$  V, 100 pA, 6 nm  $\times$  6 nm) after on-surface oligomerization. Rationalization of the different observed reaction pathways (annealing temperature  $123$ – $140^\circ\text{C}$ ) and the corresponding molecular structures. b) Statistical analysis for the distribution of the observed products on Au(111).

portion of  $(10.7 \pm 3.1)\%$  and bond formation according to “other” pathways occurred to a small extent  $((3.6 \pm 2.4)\%)$ .

All identified reaction pathways may lead to the construction of novel interfacial networks. However, here we focus on the optimization of the process towards highly selective Glaser coupling (pathway I) for the controlled on-surface synthesis of linear conjugated polymer chains.

We first investigated the influence of the structure of the metal surface on the oligomerization of **1** by switching to the Au(100) surface to achieve enhanced selectivity for formation of long polymer chains (suppression of chain branching). However, after the substrate had been covered with alkyne **1** and annealed, the surface reaction did not show a better selectivity and shorter chains were formed (for STM images see the Supporting Information).

Other substrates such as Cu(111) and Ag(111) were also investigated. As the Glaser coupling in solution is mediated by copper complexes, it is worth considering Cu(111) as a solid substrate for the 2D Glaser coupling. We observed the desired homocoupling reaction for alkyne **1** and obtained oligomeric chains (see the Supporting Information). However, selectivity towards the linear chains was low and many branching points were identified. In contrast, we found that the Ag(111) surface exhibits high selectivity towards Glaser coupling. Alkyne **1** deposited on the Ag(111) surface formed highly ordered monolayers. Subsequent annealing of the **1**-covered Ag(111) surface provided oligomeric structures with up to 15 monomer units in a row (Figure 3a). For a more quantitative analysis of the reaction outcome we performed

a statistical analysis of the different reaction modes as described above (Figure 3b).

We found that the two-unit linear coupling I/II at Ag(111) showed a relative abundance of up to  $(64.3 \pm 8.1)\%$ . This was far higher than the proportion obtained on the Au(111) surface. Consequently, the occurrence of reaction pathways III, IV/V, VI, and “other” was significantly reduced to  $(4.6 \pm 0.6)\%$ ,  $(19.7 \pm 5.7)\%$ ,  $(6.8 \pm 1.9)\%$ , and  $(4.6 \pm 0.9)\%$ , respectively. Hence, oligomerization of **1** for the generation of  $\pi$ -conjugated linear chains by Glaser coupling is much more efficient on Ag(111) than on Au(111) surfaces.

To further improve the selectivity towards reaction pathway I, we next varied the substitution pattern of the bisalkynylarene monomer. An *ortho* substituent next to the alkyne functionality should slow down the side reactions for steric reasons and we therefore prepared alkyne **2** (Figure 4a; for the preparation see the Supporting Information). Deposition of alkyne **2** on Au(111) gave a highly ordered monolayer on the metal interface over a large area (Figure 4b) with the alkyne groups of isolated molecules in close proximity.

The measured length along the alkyne axis was 1.00 nm and length along the alkyl side chains was 2.01 nm. The parameters for the periodic cell were: *a* 1.37 nm, *b* 1.03 nm with an angle of  $101^\circ$ . Annealing of the molecular layer of **2** on Au(111) led to 2D homocoupling yielding short linear polymer chains as shown in Figure 4c. Moreover, we compared the experimental center-to-center distance of linear linked molecules of type **2** with the theoretical bond length obtained by DFT calculations. The resulting distances are in very good agreement (experimental value:  $(0.93 \pm 0.01)$  nm; theoretical value: 0.95 nm). Again, the possible C-Au-C linkage resulting in a calculated center-to-center distance of 1.20 nm could be excluded.

In analogy to the study of the reaction outcome with alkyne **1**, we compiled a statistical distribution for all reactions occurring on the Au(111) surface by analyzing intermolecular connections (Figure 4c,d). The coupling of **2** on Au(111) showed a strongly enhanced selectivity towards the formation of the targeted linear chains with a frequency of  $(92.1 \pm 5.2)\%$ , while reactions following pathways IV/V were completely suppressed (Figure 5a). Reactions III  $((2.6 \pm 0.9)\%)$  and VI  $((2.2 \pm 2.7)\%)$  were also largely reduced. This statistical analysis indicates that when one *ortho* position next to the reacting alkyne moiety is blocked with an alkyl substituent, the Glaser coupling becomes the major reaction pathway and good selectivity results.

A further improvement of the on-surface oligomerization was achieved by performing the alkyne coupling reaction with **2** on an Ag(111) surface (Figure 4e,f). In this case, both the structure of the molecules and the effect of the surface made the Glaser coupling the preferred reaction among the various processes shown in Figure 2a. Annealing of the Ag(111) surface covered with **2** at  $125^\circ\text{C}$  led to gradual chain growth and within 30 min we observed polymeric chains with high selectivity; the longest chains contain 59 precursor units (little branching, Figure 4e). Growth of monomer **2** at the hot clean surface could further lead to larger conjugated polyalkyne islands. The main reaction pathway was the Glaser homo-

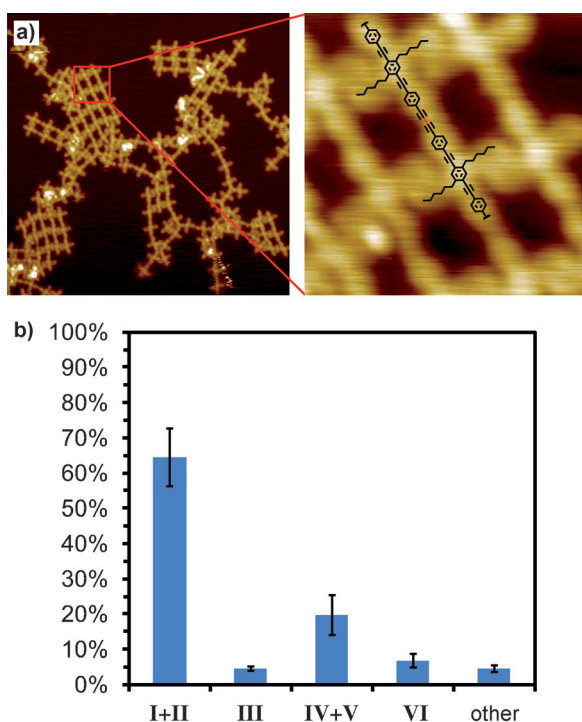


**Figure 3.** a) STM images of alkyne **1** on Ag(111) after on-surface oligomerization ( $-2$  V, 10 pA,  $40\text{ nm} \times 40\text{ nm}$ , area of inset  $5\text{ nm} \times 5\text{ nm}$ ). b) Statistical analysis for the distribution of the observed products on Ag(111).



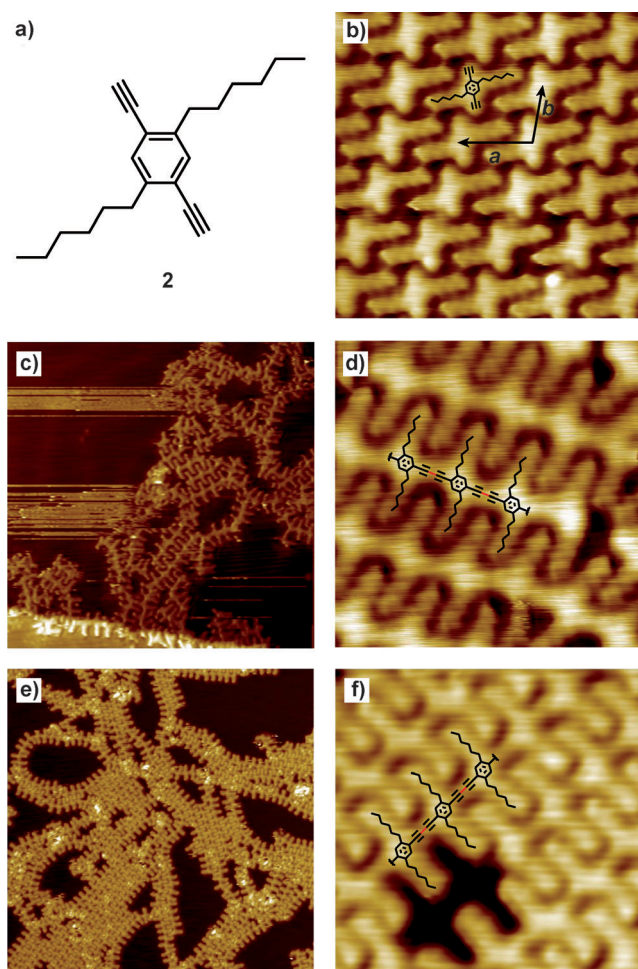


**Figure 4.** a) Molecular structure of alkyne **2**. b) High-resolution STM image of alkyne **2** on Au(111) (0.5 V, 100 pA, 6 nm × 6 nm). c) and d) STM image and high-resolution image of **2** on Au(111) after annealing (0.5 V, 100 pA, 25 nm × 25 nm and 5 nm × 5 nm). e) and f) STM image and high-resolution image of **2** on Ag(111) after annealing (0.5 V, 50 pA, 40 nm × 40 nm and 5 nm × 5 nm).

coupling occurring with a frequency of  $(96.4 \pm 1.7)\%$ . The abundance of reaction pathways III and VI was further reduced to  $(0.8 \pm 0.4)\%$  and  $(1.7 \pm 0.8)\%$ , respectively (Figure 5b).

The optimization of the 2D Glaser coupling indicated that both the *ortho* substituents at the arene next to the alkyne moiety in the organic template and also Ag(111) as a solid substrate are important for achieving the selective and efficient coupling of alkynes at the interface. Based on generally accepted mechanisms of Glaser-type couplings,<sup>[12a]</sup> we assume that annealing of the surface-assembled monomers leads to alkynyl–metal intermediates at the interface, which undergo reductive coupling to give the Glaser product. We believe that the different binding energies of the precursor molecules to the solid substrate rationalize the surface-dependent selectivity towards the Glaser coupling reaction of the alkynes.

In summary, we have showed that the Glaser coupling can be used highly efficiently to generate linear oligomer/polymer

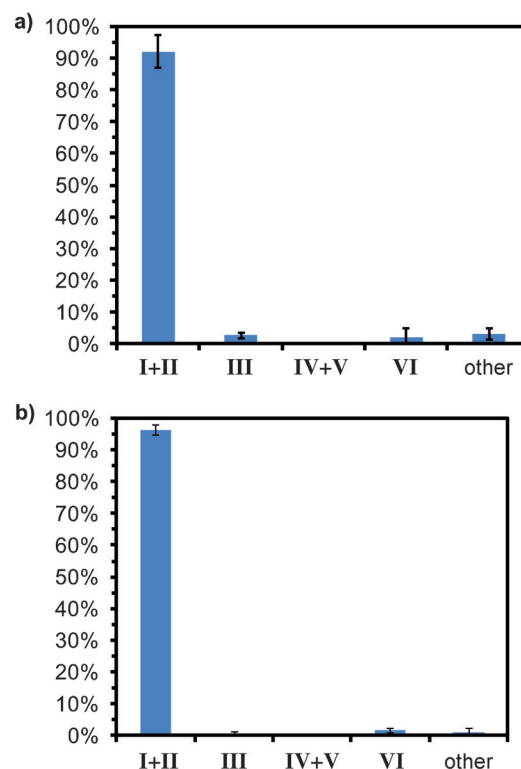


**Figure 5.** Statistical analysis for the distribution of observed products from reactions of **2** on a) Au(111) and b) Ag(111).

chains in spatial confinement at surfaces, which is impossible in conventional solution schemes. The generation of  $\pi$ -conjugated linear polymers directly at the interface is possible by using appropriate precursors and subsequent on-surface coupling. It turned out that the Glaser coupling is more efficient on Ag(111) surfaces than on Au(111) and Cu(111). The surface acts as a 2D supporting system allowing the molecules to adsorb and orient in two-dimensional space, and it also likely mediates the reactions. The substitution pattern of the organic precursor molecules is also of great importance and simple steric shielding of the alkyne led to the suppression of side reactions. We believe that the approach presented herein is not restricted to the formation of  $\pi$ -conjugated linear chains but is also appropriate for the formation of defined  $\pi$ -conjugated two-dimensional networks.

## Experimental Section

Experiments were performed with a UHV low-temperature STM (Omicron) at a base pressure of  $1 \times 10^{-10}$  mbar, which operates at 78 K in the constant-current topographic mode. The bias is the sample voltage with respect to the STM tip. Atomic flat single-crystalline metal surfaces were cleaned by cycles of ion sputtering and annealing. Alkyne **1** was evaporated in UHV by sublimation from a Knudsen cell at roughly 150 °C onto the metal surface by using organic molecular beam deposition (OMBD). The deposition rate, approximately  $0.04 \text{ ML min}^{-1}$  (monolayers per minute), was calibrated from the STM images. Alkyne **2** with a relatively high vapor pressure at room temperature was deposited onto the metal surface by free diffusion using a custom-designed funnel in an isolated chamber (the funnel was made of aluminum foil to hold a small quartz tube containing **2**).

The deposition rate,  $1.2 \text{ ML min}^{-1}$ , was calibrated from the STM images. The annealing process for the coupling reaction was monitored by an IR thermometer.

Received: October 25, 2012

Published online: February 19, 2013

**Keywords:** C–C coupling · conjugation · polymerization · scanning tunneling microscopy · surface chemistry

- [1] a) A. Gourdon, *Angew. Chem.* **2008**, *120*, 7056–7059; *Angew. Chem. Int. Ed.* **2008**, *47*, 6950–6953; b) D. F. Perepichka, F. Rosei, *Science* **2009**, *323*, 216–217; c) J. A. A. W. Elemans, S. Lei, S. De Feyter, *Angew. Chem.* **2009**, *121*, 7434–7469; *Angew. Chem. Int. Ed.* **2009**, *48*, 7298–7332; d) C.-A. Palma, P. Samori, *Nat. Chem.* **2011**, *3*, 431–436; e) J. Sakamoto, J. von Heijst, O. Lukin, A. D. Schlüter, *Angew. Chem.* **2009**, *121*, 1048–1089; *Angew. Chem. Int. Ed.* **2009**, *48*, 1030–1069.
- [2] S. W. Hla, L. Bartels, G. Meyer, K. H. Rieder, *Phys. Rev. Lett.* **2000**, *85*, 2777–2780.
- [3] a) L. Grill, M. Dyer, L. Lafferentz, M. Persson, M. V. Peters, S. Hecht, *Nat. Nanotechnol.* **2007**, *2*, 687–691; b) L. Lafferentz F. Ample, H. Yu, S. Hecht, C. Joachim, L. Grill, *Science* **2009**, *323*, 1193–1197; c) A. Saywell, J. Schwarz, S. Hecht, L. Grill, *Angew. Chem.* **2012**, *124*, 5186–5190; *Angew. Chem. Int. Ed.* **2012**, *51*, 5096–5100.
- [4] a) M. Bieri, M. Treier, J. Cai, K. Ait-Mansour, P. Ruffieux, O. Gröning, P. Gröning, M. Kastler, R. Rieger, X. Feng, K. Müllen, R. Fasel, *Chem. Commun.* **2009**, 6919–6921; b) M. Bieri, S. Blankenburg, M. Kivala, C. A. Pignoli, P. Ruffieux, K. Müllen, R. Fasel, *Chem. Commun.* **2011**, *47*, 10239–10241; c) M. Bieri, M.-T. Nguyen, O. Gröning, J. Cai, M. Treier, K. Ait-Mansour, P. Ruffieux, C. A. Pignedoli, D. Passerone, M. Kastler, K. Müllen, R. Fasel, *J. Am. Chem. Soc.* **2010**, *132*, 16669–16676; d) J. Cai, P. Ruffieux, R. Jaafar, M. Bieri, T. Braun, S. Blankenburg, M. Muoth, A. P. Seitsonen, M. Saleh, X. Feng, K. Müllen, R. Fasel, *Nature* **2010**, *466*, 470–473.
- [5] a) L. Lafferentz, V. Eberhardt, C. Dri, C. Africh, G. Comelli, F. Esch, S. Hecht, L. Grill, *Nat. Chem.* **2012**, *4*, 215; b) N. R. Champness, *Nat. Chem.* **2012**, *4*, 149–150.
- [6] a) S. Weigelt, C. Busse, C. Bombis, M. M. Knudsen, K. V. Gothelf, T. Strunskus, C. Wöll, M. Dahlboom, B. Hammer, E. Lægsgaard, F. Besenbacher, T. R. Linderoth, *Angew. Chem.* **2007**, *119*, 9387–9390; *Angew. Chem. Int. Ed.* **2007**, *46*, 9227–9230; b) S. Weigelt, C. Bombis, C. Busse, M. K. Knudsen, K. V. Gothelf, E. Lægsgaard, F. Besenbacher, T. R. Linderoth, *ACS Nano* **2008**, *2*, 651–660; c) S. Weigelt, C. Busse, C. Bombis, M. M. Knudsen, K. V. Gothelf, E. Lægsgaard, F. Besenbacher, T. R. Linderoth, *Angew. Chem.* **2008**, *120*, 4478–4482; *Angew. Chem. Int. Ed.* **2008**, *47*, 4406–4410.
- [7] N. A. A. Zwaneveld, R. Pawlak, M. Abel, D. Catalin, D. Gigmes, D. Bertin, L. Porte, *J. Am. Chem. Soc.* **2008**, *130*, 6678–6679.
- [8] M. Matena, T. Riehm, M. Stähr, T. A. Jung, L. H. Gade, *Angew. Chem.* **2008**, *120*, 2448–2451; *Angew. Chem. Int. Ed.* **2008**, *47*, 2414–2417.
- [9] M. Treier, N. V. Richardson, R. Fasel, *J. Am. Chem. Soc.* **2008**, *130*, 14054–14055; b) A. C. Marele, R. Mas-Ballesté, L. Terracciano, J. Rodríguez-Fernández, I. Berlanga, S. S. Alexandre, R. Otero, J. M. Gallego, F. Zamora, J. M. Gómez-Rodríguez, *Chem. Commun.* **2012**, *48*, 6779–6781.
- [10] D. Zhong, J.-H. Franke, S. K. Podiyanachari, T. Blömker, H. Zhang, G. Kehr, G. Erker, H. Fuchs, L. Chi, *Science* **2011**, *334*, 213–216.
- [11] a) C. Glaser, *Ber. Dtsch. Chem. Ges.* **1869**, *2*, 422–424; b) C. Glaser, *Ann. Chem. Pharm.* **1870**, *154*, 137–171.
- [12] a) P. Siemsen, R. C. Livingston, F. Diederich, *Angew. Chem.* **2000**, *112*, 2740–2767; *Angew. Chem. Int. Ed.* **2000**, *39*, 2632–2657; b) N. C. Greenham, S. C. Moratti, D. D. C. Bradley, R. H. Friend, A. B. Holmes, *Nature* **1993**, *365*, 628–630; c) J. L. Brédas, *Adv. Mater.* **1995**, *7*, 263–274; d) C. C. C. Johansson Seechurn, M. O. Kitching, T. J. Colacot, V. Snieckus, *Angew. Chem.* **2012**, *124*, 5150–5174; *Angew. Chem. Int. Ed.* **2012**, *51*, 5062–5085.